Sensors and Actuators B 248 (2017) 973–979

Contents lists available at ScienceDirect

Sensors and Actuators B: Chemical

journal homepage: www.elsevier.com/locate/snb

Detection of protein kinase using an aptamer on a microchip integrated electrolyte-insulator-semiconductor sensor

Rohit Chand [a,b], Dawoon Han [a], Suresh Neethirajan [b], Yong-Sang Kim [a,*]

[a] School of Electronic and Electrical Engineering, Sungkyunkwan University, Suwon, Gyeonggi, 16419, South Korea
[b] BioNano Laboratory, School of Engineering, University of Guelph, Guelph, Ontario, N1G 2W1, Canada

ARTICLE INFO

Article history:
Received 15 October 2016
Received in revised form 22 January 2017
Accepted 22 February 2017
Available online 24 February 2017

Keywords:
Aptamer
Biosensor
Capacitance
Electrolyte-insulator-semiconductor
Microchip
Protein kinase A

ABSTRACT

Herein, we developed a microchip electrolyte-insulator-semiconductor (EIS) sensor for the capacitive detection of protein kinase A (PKA). EIS sensing is customarily performed in a Teflon cell to define the sensing area. However, in this work, a rapid prototyping technique was followed to integrate polymeric microchip, a reference electrode, and the EIS sensor. The aptameric peptide was used for one-step and label-free detection of PKA enzyme. The thiolated PKA-specific aptamer was immobilized on the gold nanoparticles decorated EIS sensor surface. The detection of PKA in microchip was based on the change in surface charge of EIS sensor. We also analyzed the ability of microchip-EIS sensor to distinguish between buffers at different pH. An average sensitivity of 96 mV/pH for a pH range of 5–9 was obtained. The quantitative detection of PKA was performed by analyzing the capacitance-voltage curve after the aptamer-PKA interaction. The EIS sensor showed a detection limit of 2 U/mL with a relative linearity from 10 U/mL to 80 U/mL for the detection of PKA. This study proposes an integrated and point-of-care applicable biosensor for the rapid diagnosis.

1. Introduction

Protein kinases are enzymes that mediate the transfer of a phosphate group from adenosine triphosphate to a target protein, thus monitoring the cellular life. Regulation of protein function through phosphorylation is an important part of the post-translational modification. Altering the phosphorylation of intracellular proteins is a common mode of action of many toxins and pathogens. Several medical conditions, including cancers, Alzheimer's, and autoimmune diseases are linked to irregular phosphorylation of protein [1,2]. The extracellular protein kinase A level rises up to 20 U/mL, whereas the total kinase concentration is much higher in the cancer patients [3]. Therefore, determination of protein kinase is crucial in terms of biochemical diagnosis.

Conventional techniques like radioisotope labeling, mass spectroscopy, or enzyme-linked immunosorbent assays based kinase detection consume many expensive and hazardous reagents and typically require long durations for analysis [4,5]. Additionally, miniaturization of these techniques for the point-of-care use is quite not possible. Electrochemical and optical based detection are modern techniques and has proved to be an efficient approach [6,7]. However, most of these modern approaches depend on the kinase-catalyzed phosphorylation of peptide and require extensive labeling steps. Therefore, detection of a kinase enzyme through phosphorylation of peptide, involving multiple washing, incubation, reaction, and detection sequence is time-consuming, expensive, and laborious. Besides, use of multiple biomolecules for recognizing and reporting reduces the shelf life of biosensors.

To overcome these limitations, in our previous work, we designed one-step capacitive aptasensor on metal-insulator-semiconductor (MIS) and electrolyte-insulator-semiconductor (EIS) platforms [8]. On comparison of the two sensing platforms, we concluded that the EIS based sensors are highly sensitive for biosensing. EIS sensors are simple ion-sensitive field-effect transistors (FET) with capacitive detection [9]. EIS sensing is based on the change in gate voltage ensuing due to the release of protons (change in local pH) or intrinsic charge of the biomolecules during bio-molecular interactions [10,11]. Focusing on the isoelectric point (pI) of the biomolecule can increase or reverse the polarity of biomolecules. The change in the local surface charge modulates the space-charge of the semiconductor-insulator interface leading to a shift in the gate voltage [10].

In the last few years, a number of EIS sensors for detecting biomolecular interactions were reported which rely on the release of protons or change in the surface charge. Schoning et al. have extensively studied and reviewed the application of EIS sensors [9]. EIS

* Corresponding author.
E-mail addresses: yskim651@gmail.com, yongsang@skku.edu (Y.-S. Kim).

http://dx.doi.org/10.1016/j.snb.2017.02.140
0925-4005/

sensors have been employed to detect rheumatoid arthritis, urea, glucose, DNA amplification, and KRAS gene [12–16]. Recently, an EIS sensor for protein kinase C, ion-sensitive field effect transistor for creatine kinase II, and carbon nanotube field effect transistor for protein kinase A were reported [17–19]. Their detection depends on the time consuming kinase-catalyzed phosphorylation of peptide. In addition, these FET based sensors have a small detection range. Another drawback of these EIS sensors is the lack of an integrated microchip-based sensing platform. In the majority of EIS sensors, the sensing area is defined by a Teflon cell or patterned SU-8 structure. For the analysis, an Ag/AgCl reference electrode is inserted into buffer reservoir on the sensor surface or the total sensor is dipped in the electrolyte-containing beaker [13,15]. This makes the sensor unfit for disposable and point-of-care use. To the extent of our knowledge, only one group has developed an EIS sensor integrated with the microfluidic device for capacitive biosensing [14,20].

In this study, we developed a polymeric microchip-EIS sensor for the label-free and one-step detection of protein kinase A (PKA) using PKA-specific aptameric peptide. The EIS sensor was comprised of silicon dioxide (SiO_2) grown on the p-type silicon (Si) as the substrate. The surface of the EIS sensor was functionalized with aptamer to make it selective for the PKA and to prevent nonspecific interaction. Aptamers have attracted a considerable attention because of several advantages over antibodies [21]. Aptamers are thermally stable, easy to design and manufacture, and have unlimited applications. The fabrication of polymeric microchip follows a low cost and effortless procedure for integrating the EIS sensor. A rapid prototyping technique for a microfluidic system using polymer film and double-sided tape, in place of commonly used glass and polydimethylsiloxane, was developed to detect the PKA. The detection was based on the change in local surface charge due to aptamer-PKA interaction. Scanning electron microscopy, atomic force microscopy, Fourier transform-infrared spectroscopy, and capacitive analysis was used to study the surface modification and validation of the EIS sensor. Capacitance-voltage curves were recorded to detect the presence of PKA. As a proof of concept, we detected PKA in the spiked human cell sample. The microchip-EIS sensor benefits in a reduced reagent consumption, integrated and point-of-care analysis, and has the possibility of multiplexing with other biosensors.

2. Materials and methods

2.1. Materials

Hydrogen tetrachloroaurate(III) hydrate ($HAuCl_4{\cdot}3H_2O$), sodium citrate, 3-Mercaptopropyl)trimethoxysilane (MPTS), tris(hydroxymethyl)aminomethane (Tris), sodium chloride, and hydrochloric acid of analytical grade were purchased from Sigma-Aldrich (St. Louis, MO, USA). Polyethersulfone (PES) films were obtained from Fine chemicals (Korea). cAMP–dependent protein kinase A and protein kinase buffer was purchased from New England Biolabs (Ipswich, MA, USA) and stored at −20 °C. Thiolated aptameric peptide (Mpr-TTYADFIASGRTGRRNAIHD) was obtained from AnyGen co. Ltd (Korea). Fourier transform-infrared (FT-IR) spectra of the samples were collected between wavenumbers 400 and 4000 cm^{-1} at room temperature, using a Agilent Technologies Cary 630 FT-IR spectrophotometer coupled with an attenuated total reflectance (ATR) device. Atomic force microscopic analysis of sensor surface was performed using XE-100 (Park systems, Korea). All other reagents were of analytical grade and purchased from Sigma-Aldrich. Ultrapure de-ionized (DI) water was used throughout the experiment.

2.2. Synthesis of gold nanoparticles

The AuNPs ($d \approx 16$ nm) were synthesized using a seedless method as described before [22]. Briefly, 20 mL of 1.0 mM aqueous $HAuCl_4{\cdot}3H_2O$ solution was first brought to a boil. Next, 2 mL of 38.8 mM aqueous solution of sodium citrate was added, which was then boiled for 10 min until the color changed to deep red. The synthesized particles were characterized using UV–vis spectroscopy and scanning electrode microscope.

2.3. Fabrication of EIS sensors

p-doped silicon substrate with a resistivity of 10 W-cm was used for the fabrication of sensors. The Si wafer was cleaned using a standard Radio Corporation of America (RCA) process. A 50 nm thick SiO_2 was grown on the Si substrate through plasma-enhanced chemical vapor deposition. Next, the back of Si wafer was primed using the wafer back grinding process to obtain a 200 μm thick substrate. After priming, 100 nm thick aluminum (Al) was thermally deposited on the back of Si wafer using a vacuum thermal evaporator to serve as a back contact.

2.4. Surface functionalization of the EIS sensors

The SiO_2 surface of EIS sensor was first treated the with O_2 plasma for 5 min at 50 sccm flow rate and 5×10^{-2} Torr pressure. The O_2 plasma treatment activated the hydroxyl groups on the SiO_2 surface, which then reacts with the silane molecule. Silanization of the SiO_2 surface was performed by dipping the EIS sensor in 1% MPTS-toluene solution for 3 h. The reaction between the hydroxyl group of the EIS surface and the silane group of the MPTS formed a self-aligned monolayer, leaving free thiol group on the top. The silanized surface was thoroughly rinsed with the toluene followed by the ethanol. The EIS sensor was heated at 110 °C for 15 min to strengthen the silane bonds and activate thiol groups. Next, the synthesized AuNPs were allowed to anchor on the MPTS modified EIS sensor for 6 h. The reaction between thiol groups of the MPTS and Au captured the AuNPs on the EIS sensor. The AuNPs modified EIS sensor was characterized by the scanning electron microscopy and capacitance–voltage (C–V) analysis. The functionalization of the EIS sensor was finalized after immobilizing the aptamer solution on the AuNPs for 6 h at 4 °C.

2.5. Fabrication of EIS microchip

The rapid prototyping technique for microchip based on a polymer film and the double-sided tape was employed (Fig. 1(a)). The fabrication technique was adopted from the previously reported works [1,23]. For this purpose, we used polyethersulfone (PES) films and 3M™ double-sided tape. The chip was fabricated in three parts, where, the first bottom PES film layer contained the 100 nm thick Al electrode for the back contact with the EIS sensor. The aptamer functionalized EIS was bonded on the Al electrode using a thin layer of conductive silver gel. The middle double-sided tape contained the fluid network. The tape formed a reservoir with an active area of 5 mm × 5 mm. The top PES film layer contained the inlet and outlet holes for the sample. For laying the reference electrode, a shadow mask containing the electrode pattern was attached to the top PES film. Then, in a thermal vacuum evaporator, titanium layer was deposited on the PES film as an adhesion layer, followed by a layer of silver. The silver electrode was treated with 50 mM ferric chloride for 50 s followed by rinsing with DI water, to obtain a thin AgCl over the deposited Ag electrode. The three parts were aligned under a simple optical microscope and kept under pressure for 30 min. The above technique enabled a rapid prototyping of microchip without the use of a clean room facility and sophisti-

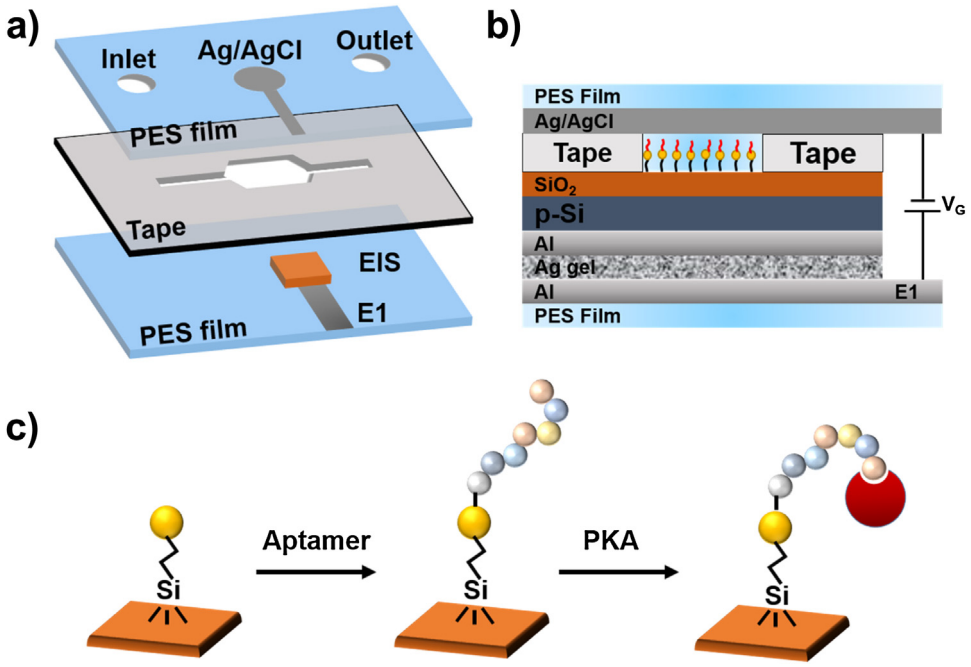

Fig. 1. (a) Schematic of the polymeric microchip, E1 = electrode for back contact, (b) Structure of the EIS sensor, and (c) Scheme of aptamer-based PKA detection on the microchip-EIS sensor.

cated instruments. The aptamer terminated EIS sensor integrated into polymeric microchip was further used for the detection of PKA.

2.6. pH sensing using microchip-EIS sensors

To verify the pH sensing ability of gold nanoparticle terminated EIS sensors, 2 mM Tris-HCl buffers with pH ranging from 5 to 9 were used. The Tris-HCl buffer was injected using a syringe into the fluid channel of the microchip and electrical response of the EIS sensor was measured for each pH. The C–V analysis on microchip-EIS was performed using a Hewlett-Packard (HP) 4284A LCR meter. The thin film Ag/AgCl electrode was used as the reference electrode. The gate voltage (V_G) was swept at a frequency of 1000 Hz with a superimposed AC signal of 10 mV.

2.7. Protein kinase A detection on microchip-EIS sensors

The one-step detection of PKA was performed by adding 10 μL of different concentrations of PKA in 1X PKA buffer on the aptamer functionalized EIS sensors. The PKA was allowed to interact with the aptamer at 25 °C. After the interaction, the reservoir was filled with 2 mM Tris-HCl buffer (pH 7) for the C-V analysis.

2.8. Detection of PKA in cell sample

Human prostate cancer cell line DU145 was obtained from American Type Culture Collection (USA). Cells were maintained in RPMI-1640 medium supplemented with 10% fetal bovine serum at 37 °C in a humidified 5% CO_2 incubator. Cells from subcultures were supplemented with 0.01% trypsin-EDTA (Sigma-Aldrich, USA) and mixed with 1X PKA buffer containing different concentrations of PKA.

3. Results and discussion

3.1. Characterization of microchip-EIS sensor

The structure of the fabricated microchip-EIS sensor is shown in Fig. 1(a). The bottom and top PES film contained electrode for the back contact and Ag/AgCl thin-film reference electrode, respectively. The tape provided fluidic connection and reservoir for the analyte and buffer during analysis. The structure of the EIS sensor is elaborated in Fig. 1(b). The EIS sensor consists of a SiO_2 layer as an active material and silicon as a semiconducting layer. A monolayer of citrate-capped AuNPs was generated on the SiO_2 film using MPTS as the linker molecule. The monolayer serves as a supporting layer for the thiolated PKA aptamer and additional gating layer. The presented fabrication methodology makes it easy to independently functionalize the EIS sensor in bulk and quickly integrate with the polymeric microchip. Each modification step of the EIS sensor surface was characterized by means of contact-angle measurements with a 12 μL drop of DI water. Fig. 3(a) presents the results of the water contact-angle measurements of a bare SiO_2 surface, O_2 plasma treated SiO_2 surface, and MPTS functionalized surface. The hydrophilicity of the surface increased significantly to a contact angle of ~7.8° after the plasma treatment from a contact angle of ~42° for a bare SiO_2. The increased surface hydrophilicity was due to the increase in hydroxyl groups. The sensor surface modified with MPTS regained the hydrophobicity (contact angle = ~37°). The change in the surface property of SiO_2 confirms the silanization of sensor. Fig. S1 shows the scanning electron microscopic analysis of EIS sensor surface to confirm the attachment of AuNPs. As evident from the image, highly resolved AuNPs with an average size of 16 ± 2 nm were attached on the SiO_2 surface. Fig. S2 shows the C-V response of EIS sensor after immobilizing negatively charged citrate-capped AuNPs. The immobilization of AuNPs altered the V_G of EIS sensor. The local charge on the surface of gate insulator affects the depletion region, thereby shifting the C-V curve of the EIS sensor. A positive shift in the V_G was seen due to the attachment of negatively charged AuNPs to the SiO_2 surface. The scheme for PKA analysis using EIS sensor is summarized in Fig. 1(c). First, the

thiolated aptamers were immobilized on the AuNPs through thiol-gold chemistry. Next, different concentrations of PKA solution in 1X reaction buffer was added to the sensor surface for interaction with the aptamer.

3.2. pH sensing using microchip-EIS sensors

The detection of PKA on microchip-EIS sensor was based on the change in the surface charge and local surface pH. Therefore, at first, we analyzed the ability of microchip-EIS sensor to distinguish between buffers at different pH. For the analysis, we fabricated EIS sensor with AuNPs terminated surface. The buffers from pH range 5–9 were injected through the microchannel and the corresponding C-V response was measured. The ionic groups present in the buffer adsorbs on the SiO_2 surface, thus changing the surface charge. This leads to a shift in the C-V curve of the EIS sensor. A response characteristic of EIS sensor at different pH buffers is shown in Fig. 2. The gate voltage (V_G) shifted towards negative and positive when the sensor surface was exposed to acidic and basic buffer, respectively. A good relationship was seen between the pH and shift in the V_G with an average sensitivity of 0.96 V/pH ($R^2 = 0.99$). This confirms the sensitivity of the microchip-EIS sensor towards the surface charge, which is useful for the PKA detection.

3.3. Optimization of experimental parameter

The concentration of aptamer is an important parameter for the detection of PKA. The aptamer used in this work was a 20 amino acid long peptide that selectively binds with the PKA [24,25]. The isoelectric point of the aptamer is around pH 9.5, therefore it is positively charged at the neutral pH value [26]. To determine the optimal concentration of aptamer that covers the surface of AuNPs monolayer, the surface was incubated with different concentration (0–200 μM) of the aptamer for 6 h. After formation of the aptamer layer, the surface was rinsed with the DI water. The shift in the C-V curve was monitored to establish the extent of deposition. As shown in Fig. S3, the immobilization of positively charged aptamer neutralized the negative charge of the AuNPs to a certain level, thus shifting the V_G towards the negative direction. The shift in the C-V curve of the microchip-EIS sensor saturated when the concentration of aptamer increased beyond 100 μM. Thus, 100 μM of aptamer was selected as the optimal for depositing on the AuNPs for further experiments.

The interaction time of the PKA and aptamer determines the performance of the EIS sensor. The optimization of reaction time was studied in the range of 0–30 min in the presence of PKA. As shown in Fig. S4, the C-V curve shifted towards the negative with the increasing reaction time, reaching a saturation at 20 min. The saturation of signal symbolizes the complete binding of the aptamer and PKA. Therefore, a reaction time of 20 min was used in the further work.

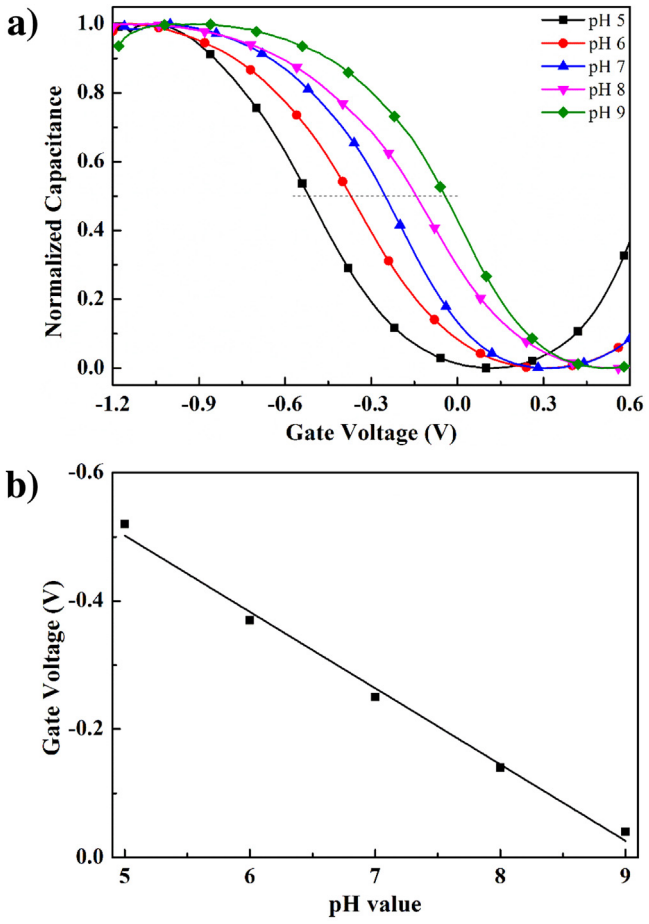

Fig. 2. The response of microchip-EIS sensor at different pH buffers w.r.t thin-film Ag/AgCl electrode: (a) C-V curves of EIS sensor at pH 5–9, (b) Relationship between pH and gate voltage. Buffer: 2 mM Tris–HCl.

3.4. Detection of protein kinase A on microchip-EIS sensors

The aptamer acts as a pseudo-substrate for the PKA enzyme, because of sequence complementarity with the binding site of the PKA. It has been extensively reported that the interaction of aptamer with the target changes the structure, total charge, and charge distribution of the aptamer [27,28]. Therefore, the EIS sensor functionalized with the kinase-specific aptamer was used for the selective, sensitive, and label-free detection of the enzyme. The AuNPs terminated EIS sensor was functionalized with 100 μm of PKA-specific aptamer and was allowed to interact with PKA for 20 min at 25 °C. The sensor surface was rinsed with DI water to eliminate the unbound PKA. The interaction of aptamer with PKA was confirmed by FT-IR spectra as shown in Fig. 3(b). The appearance of characteristic peaks of the aptameric peptide (Fig. 3(b) curve A), located at 1673 cm^{-1} (HNC═O), 1505 cm^{-1} (aromatic ring) and 1468 cm^{-1} (C—N) established the immobilization of aptamer on the gold surface. An increase in the peak intensity and presence of functional groups commonly found in the PKA enzyme confirmed the interaction and binding of aptamer with PKA (Fig. 3(b) curve B). We also performed the surface analysis of EIS sensor before and after interaction of aptamer and PKA to verify the biosensing (Fig. S5). Non-contact mode AFM topographs of the aptamer immobilized gold surface (Fig. S5(a)) and after aptamer PKA interaction (Fig. S5(b)) shows an increase in the surface roughness. In Fig. S5(b), several distinctive rough spots on the surface were apparent for the presence of aptamer-PKA complex [29,30].

For the microchip-EIS sensing of PKA, different concentrations of PKA in 1X reaction buffer was injected in the microchip and incubated with the aptamer. The pI of the PKA is pH 8.84; therefore, its interaction with aptamer further increases the positive charge on the sensor surface. This change in the charge and density on the sensor surface was recorded using C-V analysis for label-free detection of PKA. After the aptamer-PKA interaction, the reservoir was slowly filled with the tris buffer saline (TBS, 2 mM tris, 20 mM NaCl, pH 7) and then the C-V curves were analyzed. The strength of the buffer was kept low and the pH was set to 7 to reduce the effects of ions on the electrical response of the sensor.

Fig. 4(a) shows the C-V curves for label-free capacitive detection of PKA on microchip-EIS sensor. PKA solutions with a concentration range of 1–80 U/mL were detected using the proposed sensor. As can be seen from Fig. 4(a), with the increasing concentration of PKA, the V_G gradually shifted more towards the negative due

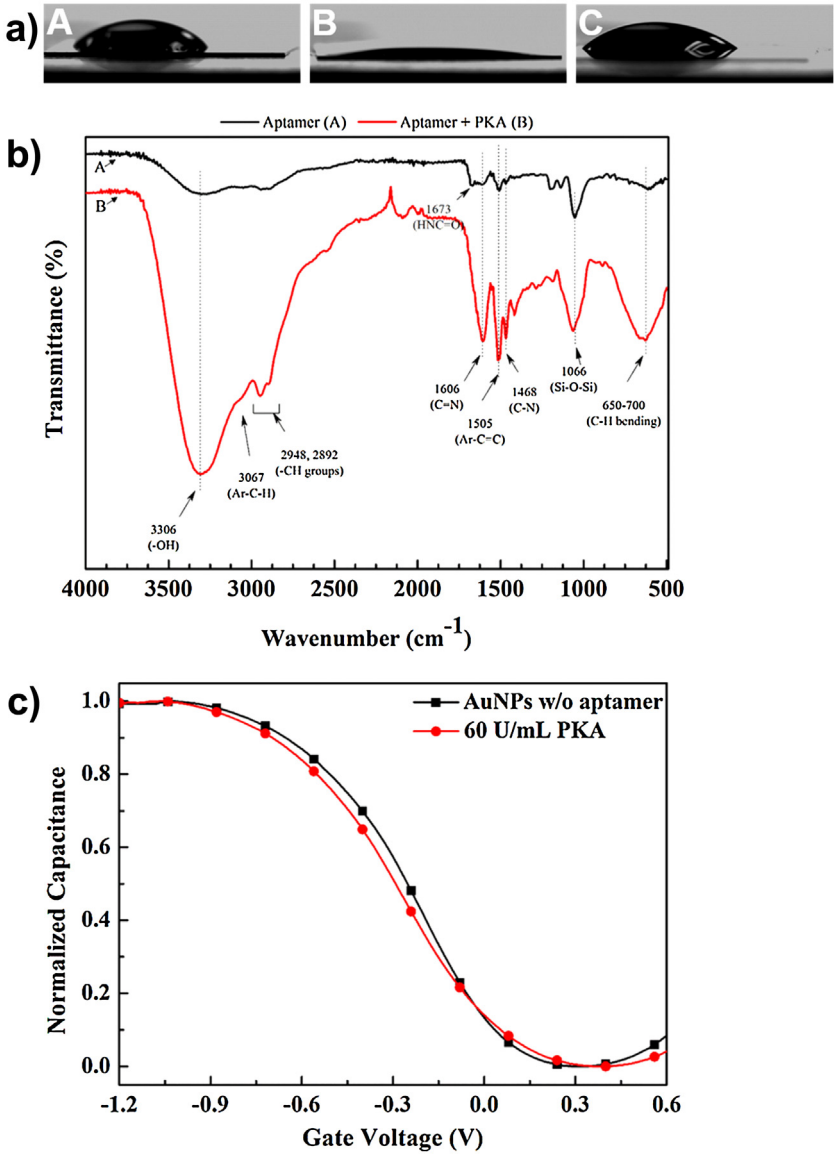

Fig. 3. Characterization of microchip-EIS sensor: (a) Water contact-angle analysis of pristine (A), O2 plasma treated (B), and MPTS immobilized (C) SiO2 surface; (b) FT-IR spectra of immobilized aptamer (A) and aptamer-PKA complex (B); (c) C-V curve for the detection of PKA without aptamer, Buffer: 2 mM Tris–HCl, pH7, using thin-film Ag/AgCl electrode.

to the change in surface charge of EIS sensor. The microchip-EIS sensor with immobilized aptamer produced a V_G of −0.451 V. Due to the interaction of aptamer with 60 U/mL of PKA, the V_G shifted to −0.775 V. Fig. 4(b) shows the response of microchip-EIS sensor with respect to the different concentration of PKA. The error bar represents the standard deviation of three independent analysis. A proportional shift in the V_G was seen with the increasing concentration of PKA. The microchip-EIS sensor showed a limit-of-detection of 2 U/mL (S/N = 3) and a relative linear range from 10 to 80 U/mL.

To prove that the obtained shift in the V_G of microchip-EIS sensor is the result of aptamer-PKA interaction only, we analyzed the PKA on AuNPs terminated sensor surface (without aptamer). The attempted detection of PKA without aptamer produced a negligible shift in the C-V curve (Fig. 3(c)). The minor shift in the C-V curve is presumably due to the electrostatic interaction of negatively charged AuNPs and positively charged PKA. However, a large shift in the V_G was observed upon interaction of aptamer and PKA (Fig. 4) which is because of the higher binding affinity of aptamer to the PKA. The lifetime of microchip-EIS sensor was investigated to study the stability of the PKA sensor. Several aptamer modified microchip-EIS sensors were stored at 4 °C for 20 days and the variation in signal was analyzed. The results demonstrated that the prepared PKA sensor has good stability and almost remained unchanged for up to 15 days (Fig. 5(a)). A ~10% decrease in the performance of microchip-EIS sensor was seen after 20 days. The specificity of the proposed aptamer functionalized microchip-EIS sensor was examined by replacing the PKA with other biological molecules. As shown in Fig. 5(b), the analysis of non-specific targets produced no noticeable change in the signal. The PKA-specific aptamer did not interact with other biomolecules, proving the specificity of the aptamer. Based on these results, we propose a microchip-EIS sensor for integrated, label-free and one-step sensing of protein kinase A.

3.5. Capacitive detection of protein kinase A in cell sample

The potentiality of the proposed microchip-EIS sensor was demonstrated by detecting PKA in the presence of human cell line.

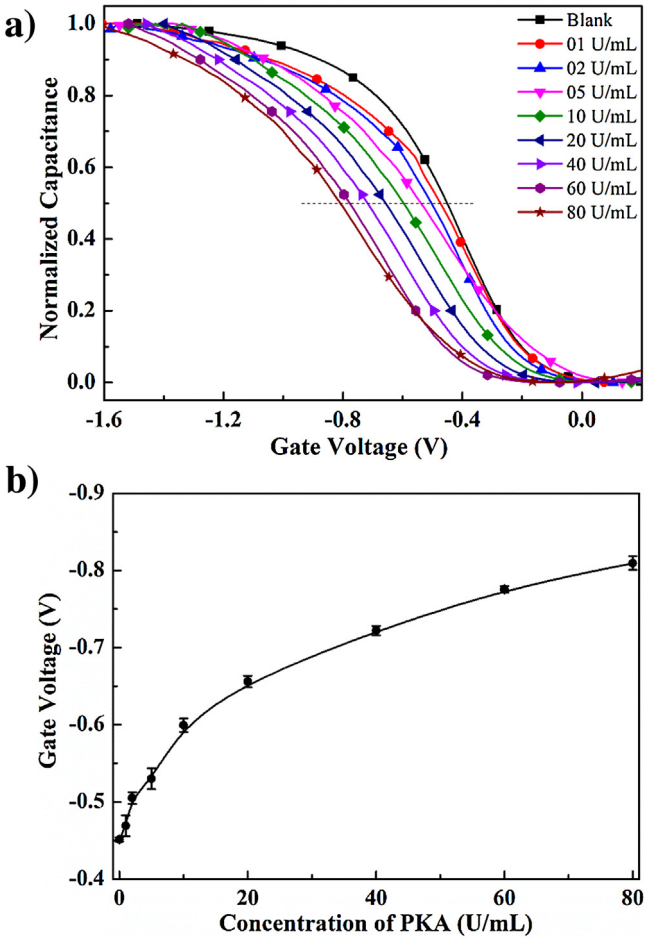

Fig. 4. The response of microchip-EIS sensor for the detection of PKA w.r.t thin-film Ag/AgCl electrode: (a) C-V curves of EIS sensor for PKA from 0 to 80 U/mL, (b) Relationship between PKA concentration and gate voltage. Buffer: 2 mM Tris–HCl, pH7.

DU145 cells in conditioned medium were spiked with the reaction mixture containing different concentrations of PKA, to simulate a biological sample. For the PKA-aptamer interaction, 10 μL of spiked cell sample was injected and incubated with the aptamer-modified microchip-EIS sensor as discussed earlier. The interaction of aptamer and PKA present in the sample was then analyzed using C-V curves. Fig. 6 summarizes the analyses, demonstrating

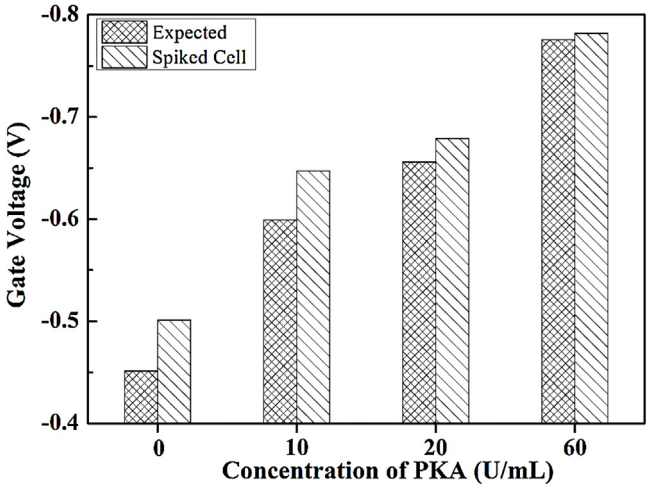

Fig. 6. Detection of PKA in the spiked human cell sample.

good recoveries with respect to the concentrations of spiked PKA. The device showed high signal to noise ratio with EIS sensor precisely distinguishing between the spiked PKA and other interfering molecules present in the medium. Therefore, the microchip-EIS sensor can be used to detect PKA in cell samples or serum from patients.

4. Conclusion

In conclusion, this work describes a strategy for development and integration of a polymeric microchip with EIS sensor for detection of PKA. The proposed sensor was highly sensitive towards the change in pH. Aptamer immobilized sensor surface facilitated in rapid biosensing. Interaction of aptamer and PKA on microchip-EIS sensor produced a shift in the gate voltage. The sensor showed a detection limit of 2 U/mL for PKA. The developed method offers attractive features like one-step detection, integrated analysis, and costless polymeric microchip. The biosensor exhibited a high response, low detection limit, and specificity towards the PKA. A polymer-based microchip makes this work beneficial for disposable and point-of-care use. The proposed sensor can also be integrated with other biosensors for multiplexed analysis.

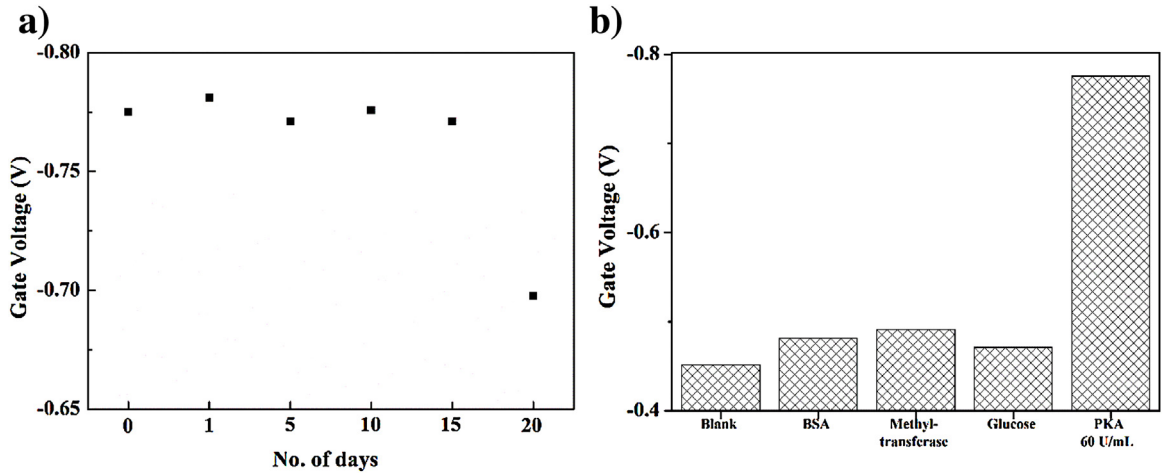

Fig. 5. The stability (a) and specificity (b) of microchip-EIS sensor, BSA = Bovine serum albumin.

Appendix A. Supplementary data

Supplementary data associated with this article can be found, in the online version, at http://dx.doi.org/10.1016/j.snb.2017.02.140.

References

[1] R. Chand, D. Han, I.-S. Shin, J.-I. Hong, Y.-S. Kim, Gold nanoparticle enhanced electrochemical assay for protein kinase activity using a synthetic chemosensor on a microchip, J. Electrochem. Soc. 162 (2015) B89–B93.
[2] A. Tedgui, Z. Mallat, Cytokines in atherosclerosis: pathogenic and regulatory pathways, Physiol. Rev. 86 (2005) 515–581.
[3] H. Wang, M. Li, W. Lin, W. Wang, Z. Zhang, E.R. Rayburn, J. Lu, D. Chen, X. Yue, F. Shen, F. Jiang, J. He, W. Wei, X. Zeng, R. Zhang, Extracellular activity of cyclic AMP-dependent protein kinase as a biomarker for human cancer detection: distribution characteristics in a normal population and cancer patients, Cancer Epidemiol. Biomark. Prev. 16 (2007) 789–795.
[4] O. von Ahsen, U. Bomer, High-throughput screening for kinase inhibitors, ChemBioChem 6 (2005) 481–490.
[5] C. D'Ambrosio, A.M. Salzano, S. Arena, G. Renzone, A. Scaloni, Analytical methodologies for the detection and structural characterization of phosphorylated proteins, J. Chromatogr. B 849 (2007) 163–180.
[6] I.-S. Shin, R. Chand, S.W. Lee, H.-W. Rhee, Y.-S. Kim, J.-I. Hong, Homogeneous electrochemical assay for protein kinase activity, Anal. Chem. 86 (2014) 10992–10995.
[7] X. Xu, X. Liu, Z. Nie, Y. Pan, M. Guo, S. Yao, Label-free fluorescent detection of protein kinase activity based on the aggregation behavior of unmodified quantum dots, Anal. Chem. 83 (2011) 52–59.
[8] R. Chand, D. Han, Y.-S. Kim, Rapid detection of protein kinase on capacitive sensing platforms, IEEE Trans. Nanobiosci. 15 (2016) 843–848.
[9] M.J. Schöning, Playing around with field-effect sensors on the basis of EIS structures, LAPS and ISFETs, Sensors 5 (2005) 126–138.
[10] T.S. Bronder, A. Poghossian, S. Scheja, C. Wu, M. Keusgen, D. Mewes, M.J. Schöning, DNA immobilization and hybridization detection by the intrinsic molecular charge using capacitive field-effect sensors modified with a charged weak polyelectrolyte layer, ACS Appl. Mater. Interfaces 7 (2015) 20068–20075.
[11] T.-W. Lina, D. Kekudaa, C.-W. Chua, Label-free detection of DNA using novel organic-based electrolyte-insulator-semiconductor, Biosens. Bioelectron. 25 (2010) 2706–2710.
[12] T.-M. Pan, T.-W. Lin, C.-Y. Chen, Label-free detection of rheumatoid factor using YbYxOy electrolyte-insulator-semiconductor devices, Anal. Chim. Acta 891 (2015) 304–311.
[13] T.-M. Pan, M.-D. Huang, W.-Y. Lin, M.-H. Wu, A urea biosensor based on pH-sensitive Sm2TiO5 electrolyte–insulator–semiconductor, Anal. Chim. Acta 11 (2010) 68–74.
[14] Y.-H. Lin, S.-H. Wang, M.-H. Wu, T.-M. Pan, C.-S. Lai, J.-D. Luo, C.-C. Chiou, Integrating solid-state sensor and microfluidic devices for glucose, urea and creatinine detection based on enzyme-carrying alginate microbeads, Biosens. Bioelectron. 43 (2013) 328–335.
[15] B. Veigas, R. Branquinho, J.V. Pinto, P.J. Wojcik, R. Martins, E. Fortunato, P.V. Baptista, Ion sensing (EIS) real-time quantitative monitorization of isothermal DNA amplification, Biosens. Bioelectron. 52 (2014) 50–55.
[16] Y.-T. Lin, A. Purwidyantri, J.-D. Luo, C.-C. Chiou, C.-M. Yang, C.-H. Lo, T.-L. Hwang, T.-H. Yen, C.-S. Lai, Programming a nonvolatile memory-like sensor for KRAS gene sensing and signal enhancement, Biosens. Bioelectron. 79 (2016) 63–70.
[17] N. Bhalla, M.D. Lorenzo, G. Pula, P. Estrela, Protein phosphorylation analysis based on proton release detection: potential tools for drug discovery, Biosens. Bioelectron. 54 (2014) 109–114.
[18] R. Freeman, R. Gill, I. Willner, Following a protein kinase activity using a field-effect transistor device, Chem. Commun. (2007) 3450–3452.
[19] C.-S. Lee, T.H. Kim, A Simple and sensitive Assay for protein kinase a using single-walled carbon nanotube Field-Effect transistor, Bull. Korean Chem. Soc. 37 (2016) 1167–1168.
[20] Y.-H. Lin, C.-H. Chiang, M.-H. Wu, T.-M. Pan, J.-D. Luo, C.-C. Chiou, Solid-state sensor incorporated in microfluidic chip and magnetic-bead enzyme immobilization approach for creatinine and glucose detection in serum, Appl. Phys. Letts. 99 (2011) 253704.
[21] K.-M. Song, S. Lee, C. Ban, Aptamers and their biological applications, Sensors 12 (2012) 612–631.
[22] J. Turkevich, P.C. Stevenson, J. Hillier, A study of the nucleation and growth processes in the synthesis of colloidal gold, Discuss. Faraday Soc. 11 (1951) 55–75.
[23] P.K. Yuen, V.N. Goral, Lab Chip 10 (2010) 384–387.
[24] H. Eldar-Finkelman, M. Eisenstein, Peptides targeting protein kinases: strategies and implications, Curr. Pharm. Des. 15 (2009) 2463–2470.
[25] D.B. Glass, H.C. Cheng, B.E. Kemp, D.A. Walsh, Differential and common recognition of the catalytic sites of the cGMP-dependent and cAMP-dependent protein kinases by inhibitory peptides derived from the heat-stable inhibitor protein, J. Biol. Chem. 261 (1986) 12166–12171.
[26] L.P. Kozlowski, IPC – Isoelectric Point Calculator, 2016. Available: http://dx.doi.org/10.1101/049841.
[27] M. Zayats, Y. Huang, R. Gill, C.-a. Ma, I. Willner, Label-free and reagentless aptamer-based sensors for small molecules, J. Am. Chem. Soc. 128 (2006) 13666–13667.
[28] M.C. Rodriguez, A.-N. Kawde, J. Wang, Aptamer biosensor for label-free impedance spectroscopy detection of proteins based on recognition-induced switching of the surface charge, Chem. Commun. (2005) 4267–4269.
[29] Y.H. Tan, J.R. Schallom, N.V. Ganesh, K. Fujikawa, A.V. Demchenko, K.J. Stine, Characterization of protein immobilization on nanoporous gold using atomic force microscopy and scanning electron microscopy, Nanoscale 3 (2011) 3395–3407.
[30] J.A.U. Paredes, A. Polini, W. Chrzanowski, Protein-based biointerfaces to control stem cell differentiation, in: D. Hutmacher, W. Chrzanowski (Eds.), Biointerfaces: Where Material Meets Biology, RSC publications, 2014, 2017, pp. 1–29.

Biographies

Rohit Chand: Rohit obtained his Ph.D. in Electronic and Electrical Engineering from Sungkyunkwan University, South Korea and M.Sc. from KIIT University, India. He has developed electrochemical and microfluidic biosensors for the detection of cancer biomarkers. Rohit worked as a post-doctoral fellow and research professor at Sungkyunkwan University, South Korea. At present, he is working as a post-doctoral fellow at BioNano Lab, University of Guelph, Canada. His research work involves micro-fabrication, surface functionalization, biosensors, and lab-on-a-chip development.

Dawoon Han: Dawoon is currently a doctoral candidate in the NEMS Lab at Sungkyunkwan University, South Korea. She completed her MS degree in Nano Science and Engineering from Myongji University, South Korea. Her research interests are in the development of electrochemical, field-effect transistor, and lab-on-a-chip based biosensors.

Suresh Neethirajan: Prof. Neethirajan is an assistant professor in Biological and Biomedical Engineering program of the University of Guelph with demonstrated research excellence and experience in large-scale multi-faceted international collaborative research projects. He is currently directing the state-of-the-art BioNano Lab and the team leader of the Precision Livestock Biosensor group at Guelph.

Yong-Sang Kim: Prof. Kim is a professor at the School of Electronic and Electrical Engineering and head of the Nano-Electronics and Microfluidic Sensors lab of the Sungkyunkwan University, South Korea. Prior to this, he was a professor in the Dept. of Electrical Engineering and director of Nano-Bio Research Centre at Myongji University, South Korea. He also served as an associate researcher at Univ. of California at Berkeley, U.S.A. Prof. Kim's research focuses on developing organic and oxide based TFTs for biological detection and use in electrical circuits. He also works on the development of microfluidic platforms for the electrochemical analysis of biomolecules and organic solar cells. He has published over 150 papers in several peer-reviewed journals.